THE JOURNAL OF BIOLOGICAL CHEMISTRY VOL. 284, NO. 40, pp. 27467–27479, October 2, 2009

Key Residues in *Mycobacterium tuberculosis* Protein Kinase G Play a Role in Regulating Kinase Activity and Survival in the Host*[S]

Received for publication, June 21, 2009 Published, JBC Papers in Press, July 28, 2009, DOI 10.1074/jbc.M109.036095

Divya Tiwari[‡1], Rajnish Kumar Singh[‡], Kasturi Goswami[‡], Sunil Kumar Verma[§1], Balaji Prakash[§], and Vinay Kumar Nandicoori[‡2]

From the [‡]National Institute of Immunology, Aruna Asaf Ali Marg, New Delhi 110067 and the [§]Department of Biological Sciences and Bioengineering, Indian Institute of Technology, Kanpur 208016, India

Protein kinase G (PknG) in *Mycobacterium tuberculosis* has been shown to modulate phagosome-lysosome fusion. The protein has three distinct domains, an N-terminal Trx domain, a kinase domain, and a C-terminal TPR domain. The present study extensively analyzes the roles of these domains in regulating PknG kinase activity and function. We find that the kinase domain of PknG by itself is inactive, signifying the importance of the flanking domains. Although the deletion of the Trx domain severely impacts the activity of the protein, the C-terminal region also contributes significantly in regulating the activity of the kinase. Apart from this, PknG kinase activity is dependent on the presence of threonine 309 in the $p + 1$ loop of the activation segment. Mutating the conserved cysteine residues in the Trx motifs makes PknG refractory to changes in the redox environment. *In vitro* experiments identify threonine 63 as the major phosphorylation site of the protein. Importantly, we find that this is the only site in the protein that is phosphorylated *in vivo*. Macrophage infection studies reveal that the first 73 residues, the Trx motifs, and the threonine 63 residue are independently essential for modulating PknG-mediated survival of mycobacteria in its host. We have extended these studies to investigate the role of PknG and PknG mutants in the pathogenesis of mycobacteria in mice. Our results reinforce the findings from the macrophage infection experiments, and for the first time demonstrate that the expression of PknG in non-pathogenic mycobacteria allows the continued existence of these bacteria in host tissues.

Protein kinases are a diverse class of proteins that have been shown to play a critical role in regulating cellular processes by transmitting extracellular cues/intracellular signals to their downstream substrates by phosphorylation of serine, threonine, or tyrosine residues on the substrates. The *Mycobacterium tuberculosis* genome encodes for 11 eukaryotic-like serine/threonine protein kinases (1). PknG is likely to be the only soluble kinase as all other kinases either have a putative transmembrane domain or are shown to be localized to the membrane fraction (2, 3). Other than PknJ, the other kinases have been biochemically characterized, and downstream target substrates of nine kinases have been identified (3–19). Many of these kinases are reported to be involved in key regulatory functions (20–24). In addition, there exists a possibility that these kinases may be involved in cross-talk with host kinases. Various studies have shown that two of these kinases, PknA and PknB, are essential for growth, and are involved in regulating cell shape (4, 25). PknF, PknH, PknD, and PknK regulate gene expression levels by phosphorylating transcription factors (3, 21, 26–28). Crystal structures of the kinase domains of PknB, PknE, and PknG as well as the sensor domain of PknD, have been determined, and all of them exhibit the typical two lobed organization observed in eukaryotic serine/threonine kinases. The N-terminal lobe contains the ATP binding site, whereas the C-terminal lobe is involved in rendering an active state and in stabilizing interactions with the substrate (29–34).

Protein kinase G (PknG)[3] is closely related to the mammalian protein kinase Cα. Unlike most *M. tuberculosis* serine/threonine protein kinases (STPKs), it does not have a transmembrane domain and has been shown to be localized to the bacterial cytosol and membrane (35). This 82-kDa protein has a Trx domain at the N terminus, a central kinase domain, and a C-terminal TPR motif. It has been shown to autophosphorylate the kinase and the C-terminal TPR domains (35). The gene encoding PknG is located in an operon with *glnH.* The inactivation of *pknG* in *M. tuberculosis* results in a 3-fold higher accumulation of glutamate and glutamine as well as reduced expression of glutamine synthetase (35). However, another report suggests that the deletion of *pknG* in *Mycobacterium bovis* BCG does not affect glutamine uptake or intracellular glutamine concentration (36). Walburger *et al.* (37) analyzed the intracellular trafficking of *pknG*-deficient *M. bovis* BCG after macrophage infection. Their data revealed rapid lysosomal transfer of phagocytosed (mutant) mycobacteria. The ortholog of PknG in *Mycobacterium smegmatis*, a non-pathogenic soil bacterium, is not expressed due to an altered ribosome binding site (8, 23). Upon infecting macrophages, wild type *M. smegmatis* is trans-

* This work was supported by the Department of Biotechnology (DBT), India (to V. K. N. and B. P.) and by an International Research Fellowship grant from the Wellcome Trust, United Kingdom (to B. P.).

[S] The on-line version of this article (available at http://www.jbc.org) contains supplemental Figs. S1–S2 and Table S1.

[1] Senior Research Fellows of the Council of Scientific and Industrial Research, India.

[2] To whom correspondence should be addressed. Tel.: 91-11-26703789; Fax: 91-11-26742125; E-mail: vinaykn@nii.res.in.

[3] The abbreviations used are: PknG, protein kinase G; STPK, serine/threonine protein kinase; MBP, maltose-binding protein; DTT, dithiothreitol; Mbp, myelin basic protein; HPLC, high pressure liquid chromatography; GFP, green fluorescent protein; CFU, colony forming unit.

ferred to lysosomal compartments, whereas *M. smegmatis* carrying overexpressed PknG is largely present in the non-lysosomal fraction of the cell (37). These results suggest a role for PknG in modulating lysosomal transfer of mycobacteria. PknG kinase activity has been shown to be essential for preventing lysosomal transfer of the phagocytosed mycobacteria. PknG was also shown to be secreted into the cytosol of host macrophages during *M. bovis* BCG infection (37). Although there is no identifiable N-terminal signal sequence for secretion in PknG, it is known that mycobacterium species have alternate secretory pathways that may aid in secretion of such molecules (38, 39). Although the essential role of an active form of PknG in *M. tuberculosis* infection has been established, there are no reports to date regarding the exact mechanism involved. *M. tuberculosis* PknG shares about 45% identity and 59% homology with corynebacterial PknG (CgPknG), its ortholog in *Corynebacterium glutamicum*. CgPknG is not autophosphorylated, but rather, is transphosphorylated by another kinase, CgPknA. This transphosphorylation at the C-terminal domain is essential for the activity of the protein and also the phosphorylation of its downstream substrate (40). However, in *M. tuberculosis,* PknG has been reported to be autophosphorylated *in vitro*, signifying mechanistic differences in the regulation of PknG and CgPknG.

In this study, we have focused on deciphering the regulatory roles of the various domains of *M. tuberculosis* PknG. We have utilized GarA as the substrate in *in vitro* kinase assays, and used GarA phosphorylation as readout of PknG activity. Results of experiments with various deletion mutants of PknG show that although the N-terminal region of PknG is crucial, deleting the C-terminal region also results in loss of activity. In addition, we demonstrate that PknG is more active in an oxidizing environment rather than in a reducing environment and that Trx motifs play a role in sensing the redox environment. A major finding of this investigation is that threonine 63 (Thr-63) is a key phosphorylation site in the N-terminal domain, and is the only site phosphorylated *in vivo*. Macrophage infection experiments show that the N-terminal region of PknG, including the *in vivo* phosphorylation site Thr-63 and the Trx motifs are essential for PknG-mediated evasion of lysosomal transfer of mycobacteria in host macrophages. Results from mice infection studies with *M. smegmatis* expressing PknG or PknG mutants conclusively demonstrate a role for PknG in the persistence of pathogenic mycobacteria in its host. Most importantly, deletion of the N-terminal 73 residues, or mutating the Trx motifs, results in the abrogation of PknG-mediated survival of mycobacteria in host tissues.

EXPERIMENTAL PROCEDURES

Reagents and Radioisotopes—Restriction/modification enzymes were obtained from New England Biolabs. Cloning and expression vectors pQE2 (Qiagen) and pMAL-c2X (New England Biolabs) were purchased from the respective sources. pVV16 (an *Escherichia coli-Mycobacterium* shuttle vector) was kindly provided by TB Vaccine Testing and Research Material Contract. [γ-^{32}P]ATP (6000 Ci/mmol) was purchased from PerkinElmer Life Sciences. Inorganic [^{32}P]orthophosphate ($H_3{}^{32}PO_4$) was obtained from the Board of Radiation and Isotope Technology, Hyderabad, India. Oligonucleotide primers and analytical grade chemicals were purchased from Sigma. Sequencing of DNA was performed by MWG (India).

Protein Expression and Purification—Sequences of all the primers used and the details of all the plasmid constructs used in this study are given under supplemental Materials. Both pMAL-c2X- and pQE2-based constructs were transformed in DH5α competent cells for protein expression. Fresh transformants were grown in 500–1000 ml of LB medium containing 100 μg/ml ampicillin to a cell density of A_{600} of ~0.6. Purification of PknG was carried out as described earlier (37). For GarA purification, cultures were induced with 1 mM isopropyl 1-thio-β-D-galactopyranoside, followed by incubation at 37 °C for 5 h. His-tagged proteins were purified as described (37). Fractions were analyzed on SDS-PAGE and those containing PknG/GarA were pooled and dialyzed against a Tris-based buffer (10 mM Tris-HCl, pH 7.5, 20 mM NaCl, and 20% glycerol). Maltose-binding protein-tagged (MBP) proteins were purified following the manufacturer's recommendations (New England Biolabs). All the purified proteins were estimated and stored at −70 °C until further use.

In Vitro Kinase Assay, Phosphopeptide Maps, and Phosphoamino Acid Analysis—In vitro kinase assays were performed in a 40-μl reaction containing 25 mM HEPES-NaOH, pH 7.4, 20 mM magnesium acetate, 20 μM $MnCl_2$, 1 mM DTT, 200 μM sodium orthovanadate, 100 μM cold ATP, 10 μCi of [γ-^{32}P]ATP, and 5 pmol of GarA or other substrates such as myelin basic protein (Mbp), with or without 1 pmol of PknG or its fragments, for 10 min at 30 °C. The reactions were stopped by adding 15 μl of 4× SDS sample buffer followed by heating at 95 °C for 5 min. Reactions were resolved on 12% SDS-PAGE gels, and either transferred to nitrocellulose membrane or stained with Coomassie/silver and exposed to x-ray films for autoradiography. For quantitation, the desired bands were cut from the gels, soaked in scintillation mixture W (Spectrochem), and counts were taken using a liquid scintillation counter (Packard analyzer Tri-carb 2100 TR). Kinase assays in oxidized *versus* reduced environments were carried out as described above in the presence of 1 mM oxidized or reduced DTT, respectively. For these experiments, PknG and its mutants were purified in the absence of DTT or β-mercaptoethanol.

To determine the kinetic constants, reactions were carried out in a 40-μl volume, in 25 mM HEPES-NaOH, pH 7.4, 20 mM magnesium acetate, and 1 mM DTT, containing 50 μM cold ATP, 10 μCi of [γ-^{32}P]ATP, and 50, 125, or 250 nM PknG, PknG-(1–420), or PknG-(74–750), respectively, for 20 min at 30 °C. Concentrations of GarA in the reaction varied from 0.125 to 5 μM. The concentration (nM) of phosphorylated GarA was determined using the counts per nanomolar ATP. The rate of the phosphotransfer reaction was defined as nanomolar GarA phosphorylated/min/micromolar enzyme. K_m and V_{max} values were determined by non-linear regression analyses carried out with GraphPad prism software.

For two-dimensional phosphopeptide maps or phosphoamino acid analysis, bands corresponding to the protein(s) of interest were excised from the nitrocellulose membrane and digested with mass spectrometry grade trypsin gold (Promega). The peptides were analyzed by two-dimen-

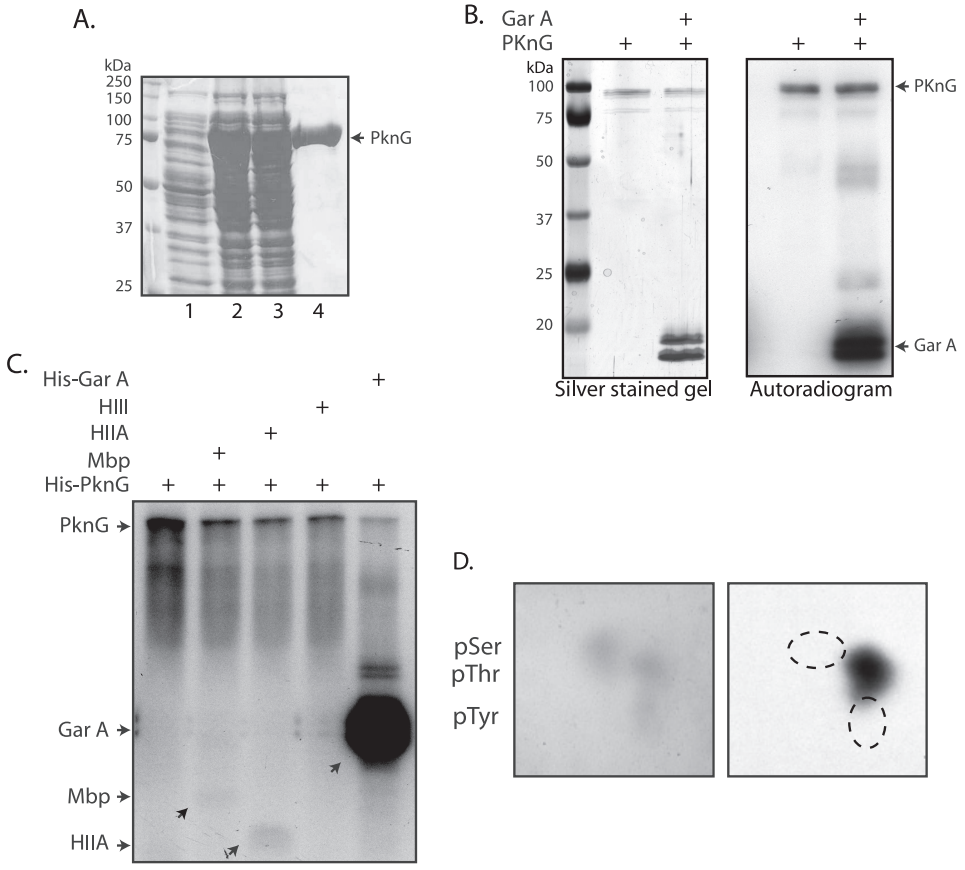

FIGURE 1. **GarA is an *in vitro* substrate of PknG.** *A*, *E. coli* DH5α cells were transformed with pQE2-PknG, and His-tagged PknG was purified as described under "Experimental Procedures." *Lane 1*, uninduced lysate; *lane 2*, induced lysate (0.1 mM isopropyl 1-thio-β-D-galactopyranoside); *lane 3*, induced lysate (1 mM isopropyl 1-thio-β-D-galactopyranoside); and *lane 4*, affinity purified His-PknG. *B*, *in vitro* kinase assays were carried out using 1 pmol of PknG with or without 5 pmol of GarA as described. These reactions were resolved on 12% SDS-PAGE, silver stained, and exposed for autoradiography. *Left panel*, silver-stained gel; *right panel*, corresponding autoradiogram. Bands corresponding to PknG and GarA are indicated by *arrows*. *C*, *in vitro* kinase reactions were carried out with 1 pmol of PknG and 5 pmol of canonical substrates or GarA as indicated. Bands corresponding to Mbp, histone HIIA, and GarA are indicated. *D*, phosphoamino acid analysis of radiolabeled PknG. *p-*, phosphorylated.

sional resolution on thin-layer cellulose plates (41). Aliquots of the tryptic peptide mixtures were further processed and phosphoamino acid analysis was carried out as described (41).

Reverse Phase-HPLC—Reverse phase-HPLC was performed using a C-18 column (PerkinElmer Life Sciences). 20 μg of Radiolabeled PknG was subjected to trypsin digestion and mixed with 200 μg of trypsin-digested PknG. This mixture was resolved by HPLC (PerkinElmer Life Sciences) using a 20–80% acetonitrile gradient. The peaks were monitored with UV as well as the radioactive detector and the peaks that were detected with the radioactive detector were collected. Two-dimensional peptide maps of these collected radioactive peaks were performed as described (41).

In Vivo Labeling of M. smegmatis—M. smegmatis harboring pVV16-PknG, pVV16-PknG-K181M, or pVV16-PknG-T63A were grown in 200 ml of Middlebrook 7H9 medium (Difco) supplemented with albumin, dextrose, and catalase and 25 μg/ml kanamycin until an O.D. of 1.5 was reached. Cells were harvested by centrifugation at 3,000 $\times$ *g* for 10 min at room temperature and washed once with phosphate-free 7H9 medium, followed by phosphate starvation in 200 ml of 7H9 phosphate-free medium for 6 h. Cells were harvested as described, and resuspended in 50 ml of phosphate-free medium containing phosphatase inhibitors (sodium orthovanadate, β-glycerophosphate, sodium fluoride, and sodium pyrophosphate) and 20 mCi of [^{32}P]orthophosphoric acid and incubated at 37 °C for 8 h at 100 $\times$ *g*. Cells were harvested and lysed using a bead beater in lysis buffer containing phosphate-buffered saline and protease inhibitors. The cell lysates were clarified by centrifugation at 15,000 $\times$ *g* for 60 min, and the supernatant was incubated with nickel-agarose beads overnight at 4 °C. The beads were then thoroughly washed with lysis buffer containing 5 mM imidazole, and resuspended in SDS sample buffer. The samples were resolved on 10% SDS-PAGE, transferred to nitrocellulose membrane, and the radiolabeled bands were visualized by phosphorimaging.

Macrophage Infection Experiments—M. smegmatis expressing green fluorescent protein (GFP) was transformed with pVV16 vector, PknG, or PknG mutants. Infection experiments were carried out as described (37) except that lysotracker red was used to detect lysosomes. Briefly, J774A.1 cells (5 $\times$ 10^5) were plated on coverslips and infected at a multiplicity of infection of 1:10 for 1 h, followed by a 3-h chase. Coverslips were removed at the given time points and stained with 0.5 μM lysotracker red diluted in Dulbecco's modified Eagle's medium for 10 min in the dark at 37 °C followed by 3 washes with phosphate-buffered saline and fixation with 4% paraformaldehyde. Coverslips were then mounted and visualized using either a Carl Zeiss Imager M1 fluorescence microscope or a Carl Zeiss Axiovision LSM510 meta confocal microscope.

In Vivo Infection with Recombinant M. smegmatis—C57BL/6J mice were obtained from The Jackson Laboratories and maintained in pathogen-free autoclaved cages in isolators. Three mice per group were injected with 2 $\times$ 10^7 colony forming units (CFU) of *M. smegmatis* (in 0.9% NaCl) transformed with pVV16 vector, PknG, or PknG mutants by intraperitoneal injection. The final inocula were diluted and plated to confirm the actual bacterial input. The survival of recombinant mycobacteria in mouse organs were determined at 2, 5, and 10 days post-infection as described (42, 43). Briefly, the mice were sacrificed and the liver, lung, and spleen were removed aseptically, and homogenized using a Down's homogenizer. The tissue homogenates were serially diluted and aliquots from each dilu-

A.

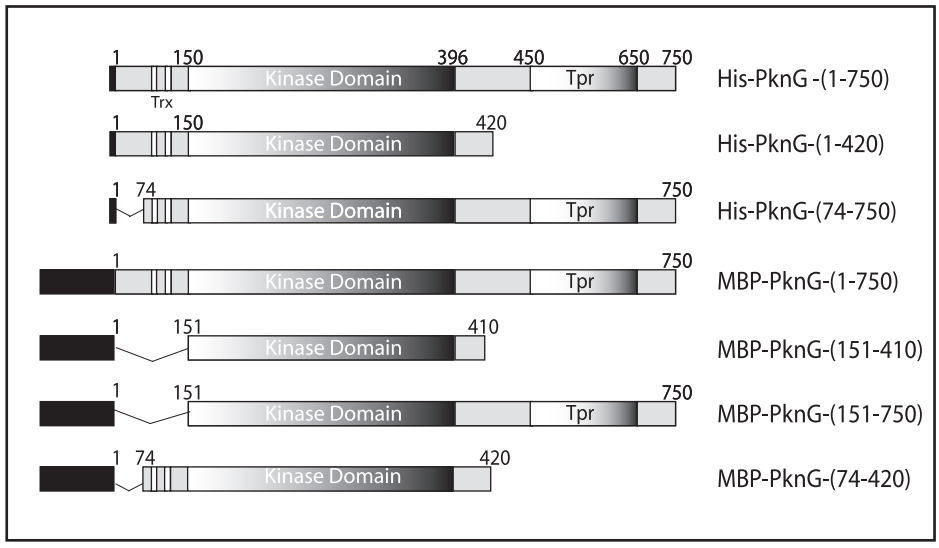

B.

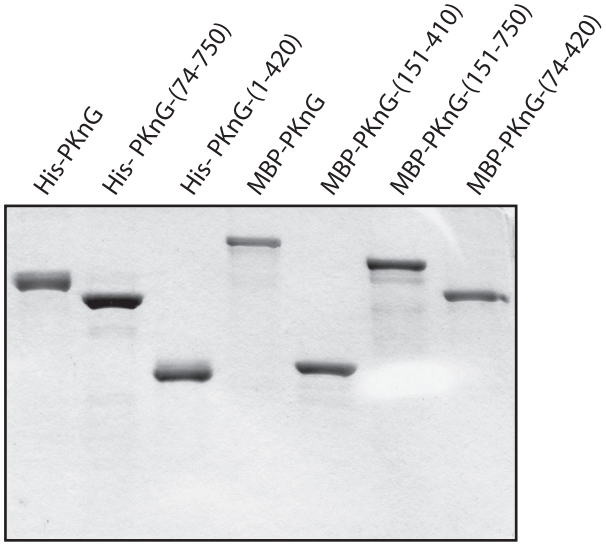

D.

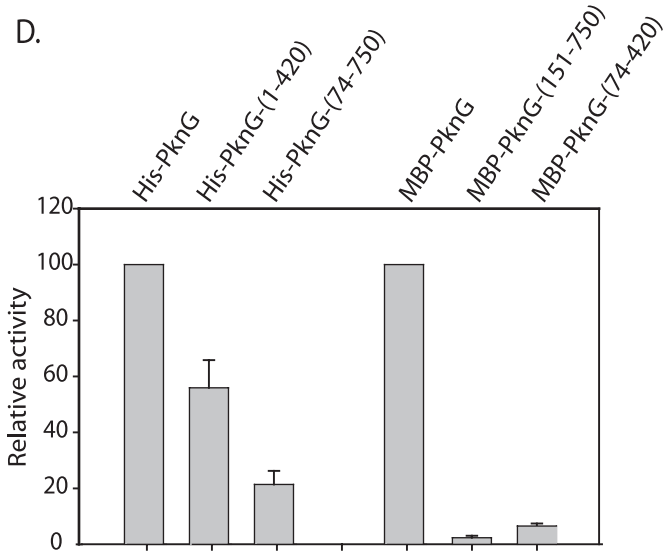

C.

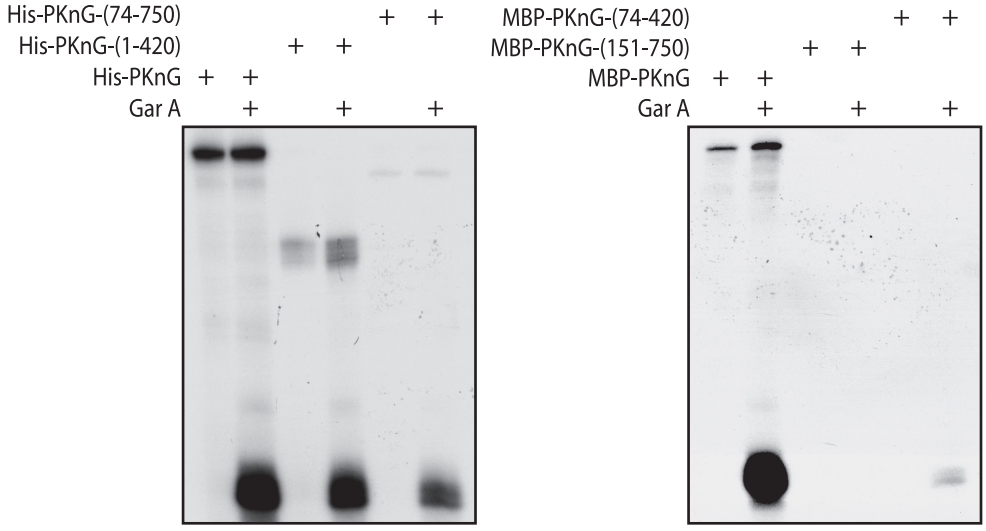

tion were plated in triplicate on Middlebrook 7H10 agar plates. Total CFUs obtained were normalized with respect to the bacterial input.

RESULTS

GarA Is an in Vitro Substrate of PknG—A comparative analysis of the proteomes of wild type and the *pknG* deletion mutant of *C. glutamicum* led to the identification of OdhI as a likely substrate of CgPknG (44). OdhI is homologous to the mycobacterial protein GarA, a protein known to be secreted in a truncated form into *M. tuberculosis* culture filtrate (CFP-17), and to induce a high interferon-γ response in inbred mice (45). This protein has earlier been identified as a substrate of *M. tuberculosis* PknB, and the PknB-mediated phosphorylation sites have been determined (46). As CgPknG and *M. tuberculosis* PknG (PknG) share a high degree of homology, we investigated the possibility of GarA being a substrate of PknG. Accordingly, the gene encoding PknG was amplified from a BAC library and cloned into pQE2 vector, and the overexpressed protein was purified to near homogeneity (Fig. 1*A*). Similarly, the gene encoding GarA (*Rv1827*) was cloned into pQE2, and overexpressed GarA was purified to homogeneity (data not shown). *In vitro* kinase assays carried out with the purified PknG using GarA as test substrate demonstrated that GarA is a substrate of PknG (Fig. 1*B*). In an earlier report, PknG was shown to phosphorylate Mbp, the universal kinase substrate (8). Interestingly, when we compared the ability of PknG to phosphorylate GarA and various canonical kinase substrates, only a weak phosphorylation of histone HIIA and Mbp was detected in comparison to the phosphorylation seen with GarA. As apparent from Fig. 1*C*, GarA is the optimal substrate among the four that were tested, and hence GarA was used as the substrate to assess PknG kinase activity in further experiments. Phosphoamino acid analysis of phosphorylated PknG showed that phosphorylation was exclusively on threonine residues (Fig. 1*D*).

The N-terminal Region of PknG Modulates Its Kinase Activity—Among the 11 kinases annotated in the *M. tuberculosis* genome, PknG is unique due to the presence of an N-terminal extension preceding the kinase domain. In the remaining STPKs, the kinase domain is located in the N terminus followed by regions that, in some of the kinases, regulate their activity (2, 47, 48). The kinase domain of PknG is located between amino acid residues 151 and 396. The 150-amino acid N-terminal region that precedes it harbors the conserved Trx motifs. The kinase domain is followed by a 354-amino acid C-terminal region showing homology to a TPR domain. To investigate the roles of these flanking regions in modulating PknG kinase activity, we created various deletion mutants of PknG (Fig. 2*A*). Analysis of proteins on SDS-PAGE showed that all are purified to near homogeneity and are stable (Fig. 2*B*). The kinase domain by itself (MBP-PknG-(151–410)) did not show any activity, suggesting the requirement of either N- or C-terminal domains or both for PknG activity (data not shown). The PknG fragment lacking the C-terminal TPR domain (PknG-(1–420)) showed significantly decreased kinase activity (Fig. 2, *C* and *D*, ~50% of wild type activity). Deleting the N-terminal 150 amino acids (PknG-(151–750)), however, resulted in the activity of PknG being critically compromised to less than 5% of the activity shown by wild type (Fig. 2, *C* and *D*). About 25% kinase activity was restored when amino acids 74–150 were reintroduced (PknG-(74–750)) (Fig. 2, *C* and *D*). Interestingly, a PknG fragment that lacks both the first 73 amino acids and the C-terminal 421–750 amino acid region (PknG-(74–420)) shows only marginal activity compared with the full-length protein. The kinetic parameters for PknG, PknG-(1–420), and PknG-(74–750) were determined. We were unable to determine the kinetic parameters for PknG-(151–750) and PknG-(74–420), as their activity was severely compromised. Results indicate (Table 1) that deletion of either the N-terminal 74 amino acids or the C-terminal region results in decreased V_{max} and increased K_m values. Although, the decrease in V_{max} was similar in both C- and N-terminal deletion mutants, the K_m seems to be more significantly altered in the case of PknG-(74–750), suggesting an important role for the N-terminal region in modulating substrate binding affinity. Taken together, our results indicate that although the N-terminal (first 150 amino acids) is absolutely essential for PknG kinase activity, the C-terminal region also plays a significant role in regulating its activity.

TABLE 1
The kinetic constants for PknG and PknG deletion mutants
Values obtained from three independent experiments were used for calculating the mean ± S.E. Kinetic constants for PknG-(74–420) and PknG-(151–750) were not determined as the activity was significantly compromised. Relative V_{max}/K_m values were calculated relative to the values obtained for reference protein PknG.

Protein	K_m	V_{max}	V_{max}/K_m	Relative V_{max}/K_m
	nM	*nM phosphate transferred/min/μM enzyme*		
PknG	2122 ± 126	102.4 ± 15.56	48	100
PknG-(1–420)	3475 ± 588	33.2 ± 6.33	9.6	20
PknG-(74–750)	6509 ± 485	22.8 ± 2.64	3.6	7.5

The Trx Motifs in the N-terminal Region of PknG Are Involved in Redox Sensing—Results in Fig. 2 clearly demonstrated that amino acids 74–150 are important in regulating PknG kinase activity and hence we set out to investigate the role played by this region. This region harbors two Trx-fold motifs ^{106}C*XX*C^{109} and ^{128}C*XX*C^{131}. Trx motifs are frequently found in thioreductases and are involved in sensing the changes in the redox potential in the microenvironment such that the activity of the proteins are modified accordingly. We hypothesized that these residues may play a similar role in PknG. Because each of the motifs contain two cysteine residues in the signature sequence, we made two double mutants, PknG-T1 (C106A, C109A) and PknG-T2 (C128A, C131A), by mutating the cys-

FIGURE 2. **The N-terminal region of PknG modulates its kinase activity.** *A*, schematic representation of PknG and PknG deletion mutants. *B*, purified PknG and PknG mutants were resolved on 10% SDS-PAGE and stained with Coomassie. *C*, comparison of kinase activities of PknG and PknG deletion mutants. *Left panel*, *in vitro* kinase assays carried out using 1 pmol of His-PknG or His-tagged PknG mutants in a 40-μl reaction with or without 5 pmol of GarA. *Right panel*, *in vitro* kinase assays carried out using 1 pmol of MBP-PknG or MBP-tagged mutants with or without 5 pmol of GarA. *D*, the relative activity of various His- or MBP-tagged PknG mutants were calculated with respect to GarA phosphorylation by His or MBP-PknG (that were set to 100%), respectively. Relative values of substrate phosphorylation with PknG mutants in three independent experiments were used to calculate the S.D. (*error bars*).

teine residues to alanine. In addition we created a combination mutant where we simultaneously mutated all four cysteine residues to alanine (PknG-T1T2). *In vitro* kinase assays using GarA as the substrate revealed that mutating either Trx domains separately decreases PknG activity by ~30%. However, the combination mutant, PknG-T1T2, showed ~25–50% activity compared with the wild type protein (Fig. 3*A* and data not shown). To examine the possibility of these motifs modulating the activity of the protein by sensing changes in the redox potential of the environment, kinase assays were performed using wild type PknG and the Trx mutant (PknG-T1T2) in the presence of 1 mM reduced DTT or oxidized DTT. Wild type PknG showed a ~2.5-fold higher activity in the oxidized environment as compared with the reduced environment (Fig. 3*B*). As expected, PknG-T1T2 showed decreased activity compared with PknG. Interestingly, we could only detect a marginal difference (~5%), if any, in the activity of this mutant in the oxidized and reduced environments. Fortuitously, both Trx motifs in PknG are flanked by tryptophan residues, which enabled us to utilize intrinsic tryptophan fluorescence spectroscopy to monitor structural changes between wild type and mutant proteins. Our results indicate that mutant PknG-T1T2 displayed a ~2-fold increase in fluorescence as compared with wild type, suggesting significant structural changes (Fig. 3*C*) in the protein. These data underline the importance of Trx motifs and the cysteine residues therein, in maintaining internal disulfide bonds. Taken together, it appears that PknG activity is modulated by the redox state of the surrounding microenvironment and the cysteine residues are critical for this phenomenon.

A Threonine Residue in the p + 1 Loop Is Crucial for PknG Activity—Kinases are known to be activated by the phosphorylation of one or more serine, threonine, or tyrosine residues in their activation loop. The activation loop comprises the region that includes the β9 helix of the kinase domain and is sandwiched between conserved DFG and APE motifs (Fig. 4*A*). Although this region is known to be variable, these residues seem to be conserved between PknB, -D, -E, and -F (Fig. 4*A*). Activation loop residues that are phosphorylated have been identified in PknB, -D, -E, and -F (indicated by an *asterisk* in Fig. 4*A*) (49). Interestingly, in the case of PknG, sequence alignment shows no conserved threonine residues in the activation loop. However, a threonine (Thr-309) is present in the *p* + 1 loop (Fig. 4*A*). The activation loop is followed by a *p* + 1 loop, which is important for kinase-substrate interactions. A threonine residue in this region is also reported to be phosphorylated in PknE (49). We determined the role of the threonine residue in the *p* + 1 loop of PknG. It can be seen from Fig. 4*B* that mutating this threonine to alanine (PknG-T309A) resulted in complete loss of PknG activity. A comparison of CD spectra obtained with PknG and PknG-T309A showed no significant difference (supplemental Fig. S1), thus precluding any gross structural changes. The loss of kinase activity of the PknG-T309A mutant could be either because the phosphorylation of this residue is essential to the activity of the protein, or alternatively, due to loss of interactions mediated through the hydroxyl group on the threonine residue. To distinguish between these two possibilities, we made mutants of PknG where Thr-309 was replaced with either a phosphomimic amino acid such as glutamate or aspartate, or with a serine residue that can provide a hydroxyl group. If the phosphorylation of Thr-309

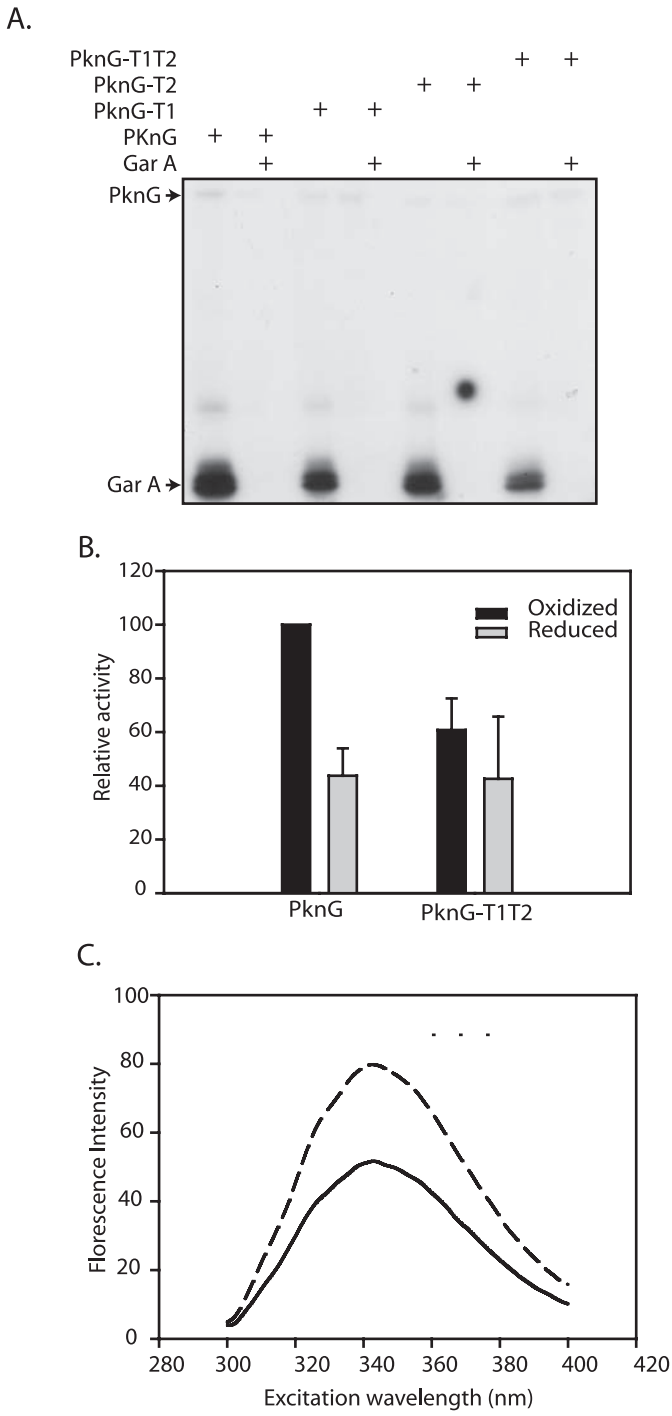

FIGURE 3. **The Trx motifs in the N-terminal region of PknG are involved in redox sensing.** *A*, *in vitro* kinase assays were carried out with PknG or PknG-T1 (^{106}*CXXC*^{109} 224 ^{106}A*XX*A^{109}) or PknG-T2 (^{128}*CXXC*^{131} 224 ^{128}A*XX*A^{131}) or PknG-T1T2 (simultaneous mutation of all four cysteine residues) with or without 5 pmol of GarA. *B*, *in vitro* kinase assays were carried out with PknG or PknG-T1T2 using 5 pmol of GarA as the substrate in the presence of 1 mM oxidized DTT or reduced DTT. Percent activity was calculated with respect to phosphorylation of GarA by PknG in the presence of 1 mM oxidized DTT. Relative values of the percent phosphorylation from three independent experiments were used for calculating the standard deviation (*error bars*). *C*, tryptophan fluorescence spectra of PknG (*solid line*) and the PknG-T1T2 mutant (*dotted line*). Fluorescence was measured after excitation at 280 nm and emission was read at 280–420 nm.

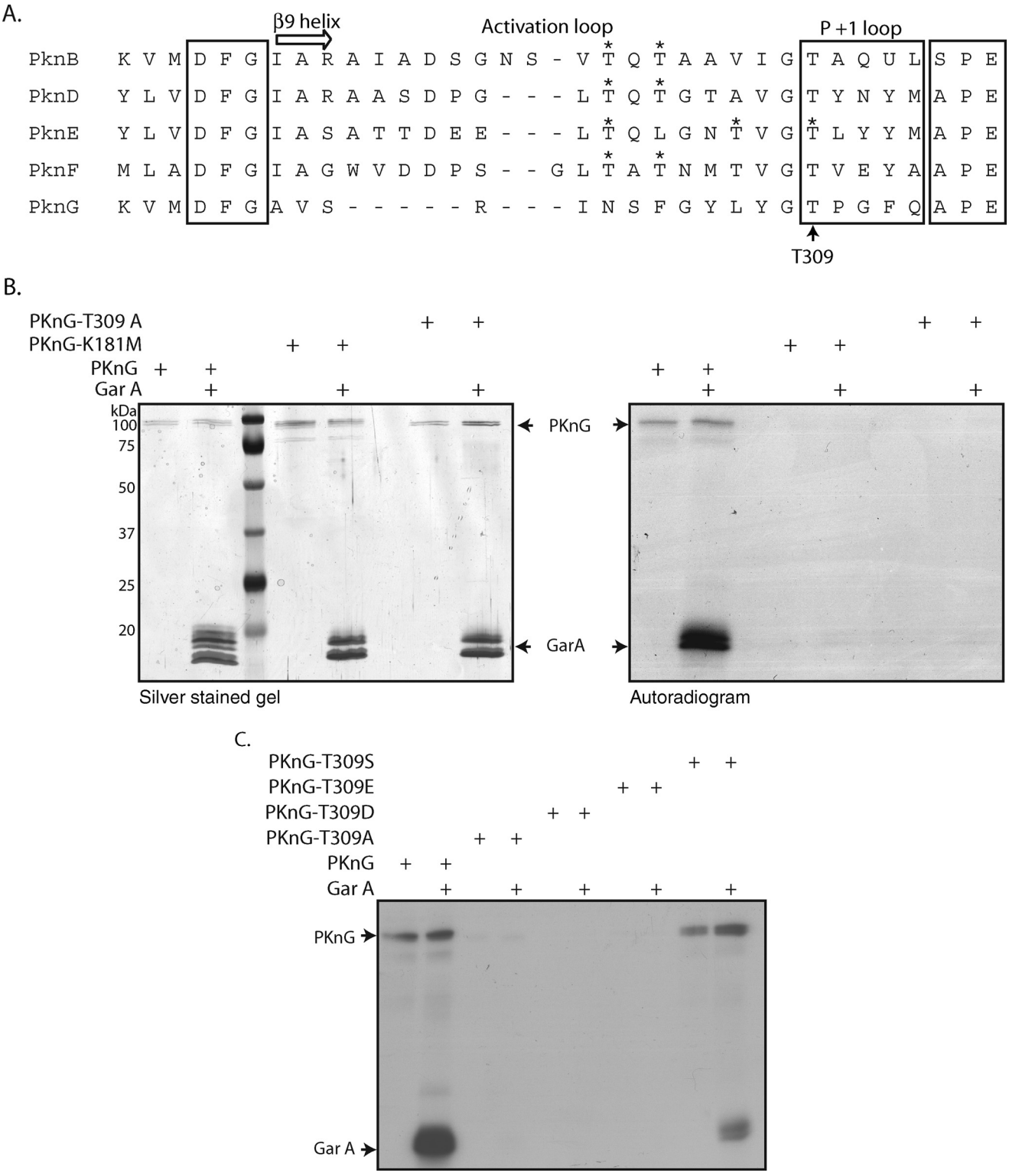

FIGURE 4. **A threonine residue in the *p* + 1 loop is crucial for PknG activity.** *A*, sequence alignment of the activation loop segment region of PknG with that of PknB, PknD, PknE, and PknF. Regions corresponding to the β9 helix, activation loop, and *p* + 1 loop are marked. Activation loop residues demonstrated to be phosphorylated in PknB, PknD, PknE, and PknF (49) are marked with an *asterisk*. *B*, *in vitro* kinase assays carried out with 1 pmol of PknG, PknG-K181M, and PknG-T309A in a 40-μl reaction with or without 5 pmol of GarA. Reactions were resolved on 12% SDS-PAGE, silver stained, and the gel was exposed for autoradiography. *Left panel*, silver-stained gel; *right panel*, corresponding autoradiogram. Bands corresponding to PknG and GarA are indicated. *C*, *in vitro* kinase assays carried out with PknG and PknG mutants using GarA as the substrate. Reactions were resolved on 12% SDS-PAGE and the gel was stained and subjected to autoradiography. Bands corresponding to PknG and GarA are indicated.

were to play a role in modulating PknG activity, T309E or T309D should be able to rescue the loss of activity of T309A. However, if the hydroxyl group of threonine plays a role, T309S should be able to restore partial activity. Our results show that both PknG T309E and T309D mutants are inactive, whereas the T309S mutant shows partial restoration of

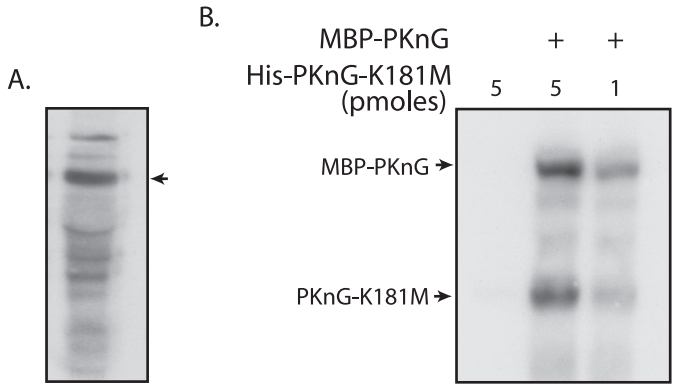

FIGURE 5. **PknG exhibits transphosphorylation.** *A*, the *PknG* gene was cloned into NdeI-HindIII sites of *M. tuberculosis* shuttle vector pVV16. *M. smegmatis* expressing pVV16-PknG was metabolically labeled and C-terminal His-tagged PknG was pulled down as described under "Experimental Procedures." The sample was resolved on 10% SDS-PAGE and transferred onto nitrocellulose membrane, and the radiolabeled bands were visualized by phosphorimaging. The radiolabeled band corresponding to PknG is indicated by an *arrow*. *B*, *in vitro* kinase assays were carried out with or without 1 pmol of MBP-PknG using either 1 or 5 pmol of PknG-K181M as substrate. Reactions were resolved on 8% SDS-PAGE, transferred onto nitrocellulose membrane, and subjected to autoradiography. Bands corresponding to His-PknG-K181M and MBP-PknG are indicated.

activity compared with the wild type (Fig. 4*C*). These data implicate a role for threonine 309 in either structural stabilization of the activation loop region or in arbitrating kinase-substrate interaction.

PknG Exhibits Trans-phosphorylation—In agreement with previous reports (8, 35), a strong phosphorylation of PknG was detected in *vitro* kinase assays (Fig. 1, *B* and *C*). To examine if the observed phosphorylation of PknG occurs *in vivo*, we overexpressed *M. tuberculosis* PknG with a C-terminal His tag in *M. smegmatis* and carried out metabolic labeling experiments with [^{32}P]orthophosphoric acid. Our results clearly show (Fig. 5*A*) that PknG is indeed phosphorylated *in vivo*. Phosphorylation of PknG could be either due to autophosphorylation or transphosphorylation, *i.e.* phosphorylation of one kinase molecule by another. To address this, we created His-tagged PknG-K181M, a mutant that lacks any kinase activity. The conserved lysine (Lys-181) present in the Walker A motif is known to stabilize ATP via interactions with α and β phosphates. Results of experiments presented in Fig. 4*B* confirm that the His-PknG-K181M mutant is indeed inactive. To discriminate between intramolecular phosphorylation *versus* intermolecular phosphorylation (*trans*-phosphorylation), we carried out *in vitro* kinase assays with wild type maltose-binding protein-tagged PknG (MBP-PknG) and His-tagged PknG-K181M mutant. The fact that we noticed a distinct phosphorylation of His-PknG-K181M, when MBP-PknG was included in the reactions (Fig. 5*B*) demonstrates that PknG phosphorylation occurs in *trans.* Although this transphosphorylation is being brought about by intermolecular interactions between PknG molecules *in vitro*, *in vivo* it may also occur due to phosphorylation by other kinases.

Threonine 63 Is a Major Phosphorylation Site in PknG—To identify the residues that are phosphorylated in PknG, we employed reverse phase-HPLC attached to a radioactive detector. Phosphorylated PknG was subjected to tryptic digestion and the resulting radiolabeled tryptic fragments were resolved on a C-18 reverse phase-HPLC column. Five distinct radioactive peaks were detected, of which peaks 1 and 5 are the major peaks (Fig. 6*A*). A comparison of the peptide maps of the wild type protein (*PknG* in Fig. 6*B*) with those for peaks 1–5 clearly indicated that all major spots with the exception of spot 6 of the wild type peptide map were accounted for in peptide maps of peaks 1–5 (Fig. 6*B*). Among the two prominent peaks, peak 1 corresponds to two major spots and peak 5 corresponds to three. As our experiments revealed that the N-terminal region is important in modulating PknG activity, we investigated possible phosphorylation of this region. To address this, we cloned and expressed the N-terminal 150 amino acids of PknG (PknG-(1–150)) fused to the His_6 tag. This protein, termed PknG-Trx, was purified and employed as a substrate in PknG kinase assays. Fig. 6*C* shows robust phosphorylation of PknG-Trx by PknG. Control PknG-Trx autophosphorylation experiments revealed that PknG-Trx does not have the ability to phosphorylate itself (data not shown). A comparison of the peptide maps of PknG and PknG-Trx showed that the latter accounts for two of the major phosphorylation sites in the PknG peptide map (Fig. 6*D*). Because phosphoamino acid analysis in Fig. 1*D* revealed that PknG exclusively phosphorylates on threonine residue(s), we individually mutagenized the 12 threonines present in PknG-Trx to alanine. To identify the phosphosphorylation site(s) we compared peptides of wild type PknG-Trx and the mutants. With the exception of PknG-Trx-T63A, the patterns of tryptic phosphopeptides of all the mutants were similar to that of PknG-Trx (data not shown). Next, we mutagenized Thr-63 to alanine in PknG, and compared the peptide map of this mutant with those of PknG, which clearly revealed the loss of two major phosphorylation spots present in PknG and PknG-Trx maps (Fig. 6*D*). These results demonstrate Thr-63 to be a major phosphorylation site in the N-terminal region. Subsequently, we assessed the role of Thr-63 in modulating PknG kinase activity. *In vitro* kinase assays carried out with purified PknG, PknG-T63A, and PknG-(74–750) showed that activity of PknG-T63A is similar to that of PknG (Fig. 7*A*). To further substantiate this observation, kinase assays were carried out with PknG, PknG-T63A, PknG-K181M, and PknG-T309A pulled down from the lysates of *M. smegmatis* expressing these proteins (Fig. 7*B*). As expected PknG-K181M and PknG-T309A were inactive. Furthermore, these results clearly demonstrate that PknG-T63A is as active as the wild type protein. To authenticate the phosphorylation site *in vivo*, wild type PknG, PknG kinase-dead mutant (K181M), and the PknG phosphorylation site mutant (T63A) were expressed as His-tagged proteins in *M. smegmatis* and metabolically labeled with [^{32}P]orthophosphoric acid. As expected, PknG was phosphorylated *in vivo* (Fig. 7*C*, *first lane*). Surprisingly, the kinase inactive mutant PknG-K181M also showed phosphorylation, perhaps indicating a transphosphorylation of PknG by another kinase in *M. smegmatis*. The most significant observation, however, is that we could not detect phosphorylation of PknG-T63A, validating *in vivo* phosphorylation of Thr-63.

The N-terminal Region of PknG Mediates the Survival of Mycobacteria in Host Macrophages—*M. smegmatis*, a non-pathogenic saprophytic species of mycobacteria, does not express PknG, and is readily transferred to lysosomes upon

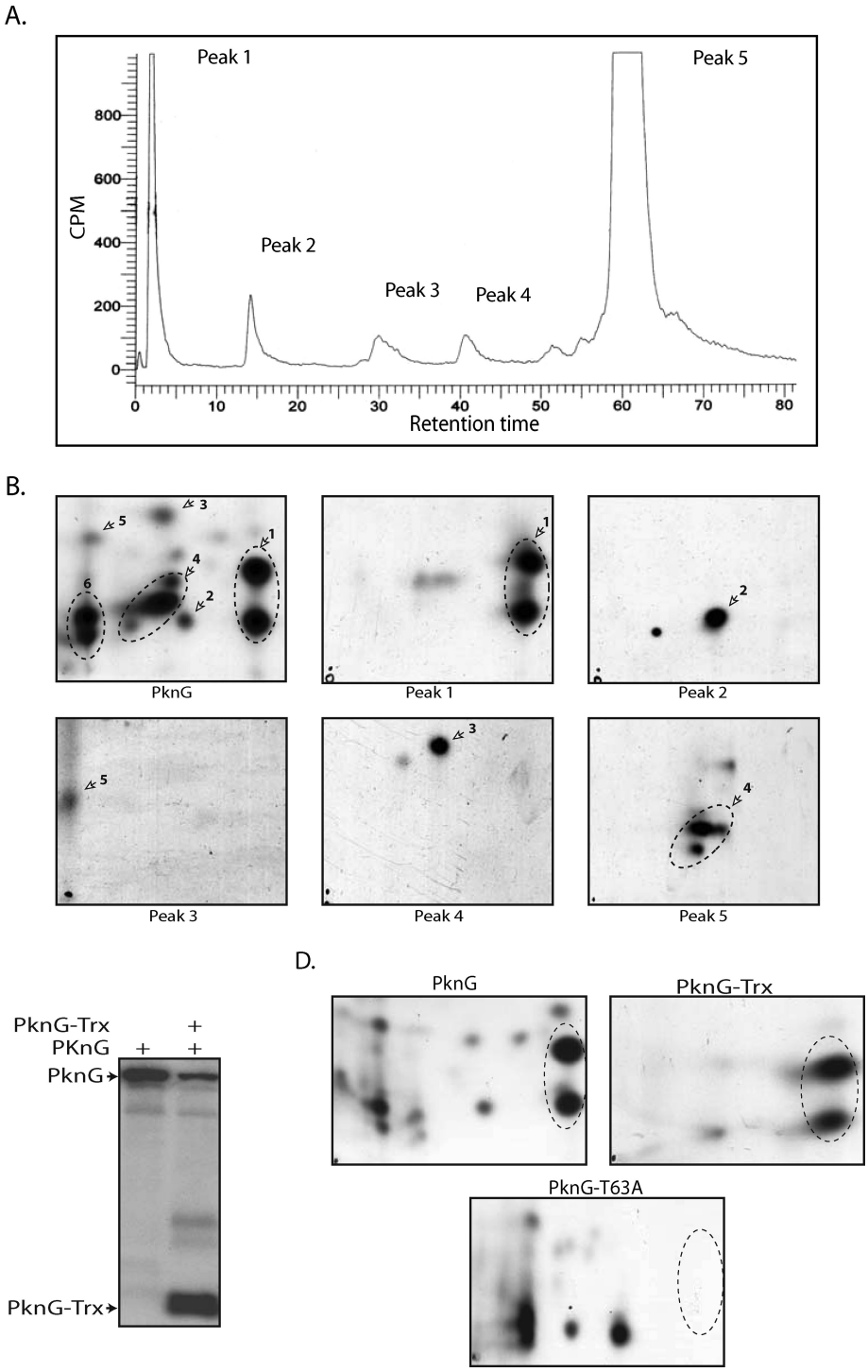

FIGURE 6. **Threonine 63 is a major phosphorylation site in PknG.** *A*, depicts the radioactive peaks eluted from the C-18 column at different retention times. *B*, aliquots of each peak were resolved by two-dimensional thin layer chromatography and the peptide maps were compared with that of wild type PknG. Spots migrating at the same positions in the peptide maps of wild type PknG and the individual peaks are *numbered* and indicated. *C*, *in vitro* kinase assays were carried out with 1 pmol of PknG in a 40-μl reaction with or without 5 pmol of PknG-Trx as the substrate. Reactions were resolved on 12% SDS-PAGE, transferred to nitrocellulose membrane, and subjected to autoradiography. Bands corresponding to PknG and PknG-Trx are indicated. *D*, *in vitro* phosphorylated PknG, PknG-Trx, and PknG-T63A were digested with trypsin, and the resulting phosphopeptides were mapped by two-dimensional resolution by thin layer chromatography. Missing phosphorylation sites in PknG-T63A are indicated by the *dotted circles*.

infection in macrophages (23, 37). Ectopic expression of PknG in *M. smegmatis* renders it resistant to clearance by macrophages. Moreover, the kinase activity of PknG is important for this phenomenon, as the expression of a kinase-dead mutant of PknG (PknG-K181M) does not confer this resistance, and the bacteria continue to be actively transfered to lysosomes (37). To address any possible role of the first 73 amino acids of PknG, especially that of the threonine 63 and Trx motifs, in the survival of mycobacteria in the host macrophages, we transformed GFP expressing *M. smegmatis* with either plasmid vector alone, or plasmids harboring PknG, PknG-K181M, PknG-(74–750), or PknG-T63A or PknG-T1T2, and infected macrophages with these transformed bacteria. Three hours post-infection, survival of *M. smegmatis* transformants was assessed by the co-localization of GFP with lysotracker red. As expected, most of the wild type *M. smegmatis* co-localized with the lysotracker red (Fig. 8). In agreement with the earlier results, *M. smegmatis* expressing PknG were able to survive outside the lysosomal compartment, and bacteria expressing PknG-K181M showed lysosomal transfer comparable with wild type *M. smegmatis* (Fig. 8) (37). The results presented here show that *M. smegmatis* expressing PknG mutants PknG-(74–750), PknG-T63A and PknG-T1T2 showed increased lysosomal transfer, implying reduced survival compared with those expressing PknG (Fig. 8). Thus, deleting the first 73 amino acids or mutating Thr-63 or the Trx motifs compromised the ability of PknG to rescue the clearance of *M. smegmatis* by macrophages. These results demonstrate a definitive role for the N-terminal 73 amino acids of PknG, Trx motifs, and the Thr-63 residue, the only phosphorylation site detected *in vivo*, in PknG-mediated prevention of lysosomal transfer of mycobacteria.

Ectopic Expression of PknG in M. smegmatis Enhances Its Persistence in Mouse Tissues—To probe the *in vivo* significance of these important observations we investigated the role of PknG and PknG mutants in pathogenesis of mycobacteria in mice. Toward this, *M. smegmatis* strains expressing pVV16 or PknG, or PknG

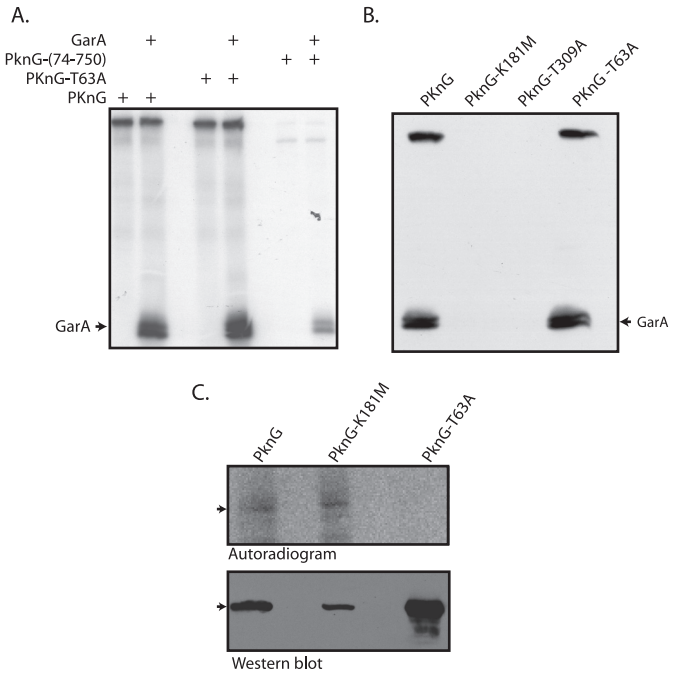

FIGURE 7. **Threonine 63 is the only phosphorylation site *in vivo*.** *A*, *in vitro* kinase assays were carried out as described using 1 pmol of PknG, PknG-T63A, and PknG-(74–750) with or without 5 pmol of GarA and 100 μM cold ATP, 10 μCi of [γ-^{32}P]ATP. *B*, His-tagged PknG or PknG-K181M, or PknG-T309A or PknG-T63A were pulled down from lysates of *M. smegmatis* strains expressing the proteins, using nickel-affinity beads. The pulled down proteins were used in *in vitro* kinase assays as described using 25 pmol of GarA and 100 μM cold ATP, and 10 μCi of [γ-^{32}P]ATP. *C*, *M. smegmatis* cells transformed with pVV16-PknG, pVV16-PknG-K181M, or pVV16-PknG-T63A were metabolically labeled and the His-tagged PknG proteins were pulled down as described under "Experimental Procedures." After resolution on 10% SDS-PAGE and transfer to nitrocellulose membrane the radiolabeled bands were visualized by phosphorimaging. The radiolabeled band corresponding to PknG is indicated by an *arrow* (*upper panel*). To determine the expression levels, the membrane was probed with αPknG rabbit polyclonal antibodies (*lower panel*).

mutants were injected intraperitoneally, and the bacterial load in liver, lungs, and spleen were analyzed by counting the CFU. Initial experiments revealed that very few bacteria localized to the lung and liver and were rapidly cleared by day 4 as compared with the spleen. Hence, further analyses were restricted only to spleen, and CFUs were determined 2, 5, and 10 days post-infection. On day 2 all the strains showed comparable CFUs signifying similar bacterial load on the spleen (Fig. 9*B*). By day 5, the spleen CFUs from mice infected with *M. smegmatis* expressing PknG showed an overall decrease, although the numbers remained significantly high as compared with the parent strain (Fig. 9*C*). In the case of mice infected with *M. smegmatis* expressing PknG-K181M (kinase dead) we noticed a significant decrease in the spleen CFUs, however, the numbers were higher than the control (Fig. 9*C*). Similar results were obtained with *M. smegmatis* strains expressing PknG-(74–750), PknG-T63A, and PknG-T1T2. By day 10, very few CFUs could be detected in the spleen of mice infected with the *M. smegmatis* strain harboring pVV16 vector or PknG-K181M, or PknG-(74–750) or PknG-T1T2 mutants (Fig. 9*D*). Interestingly, ~5-fold higher CFUs were detected in the spleen of mice infected with the *M. smegmatis* strain expressing PknG. CFUs obtained in the case of mice infected with *M. smegmatis* expressing PknG-T63A were ~2.5-fold higher than those observed for the control. However, these numbers were ~2-fold lower than those obtained with PknG.

A comparison of spleen sizes on these different days revealed a substantial splenomegaly (Fig. 9*A*) in mice infected with *M. smegmatis* expressing PknG. The mice infected with *M. smegmatis* expressing PknG mutants showed spleen sizes comparable with mice infected with wild type *M. smegmatis* (control) (Fig. 9*A*). By day 10 the spleen size in mice infected with *M. smegmatis* expressing PknG was twice the size compared with those infected with the wild type strain or the strains expressing PknG-K181M, PknG-(74–750), and PknG-T1T2 and this observation was reinforced by the fact that the spleen had higher bacterial load (Fig. 9*D*). We also observed slightly enlarged spleen in mice infected with *M. smegmatis* expressing PknG-T63A, which is in keeping with the spleen CFU count obtained on day 10. Our results for the first time demonstrate that expression of PknG in non-pathogenic mycobacteria allows the continued existence of these bacteria in host tissue.

DISCUSSION

STPKs have been shown to be involved in key regulatory functions in the organism (2, 20). This study reports the biochemical characterization of PknG and the possible functional roles of the different domains (and of specific amino acid residues therein) in regulating kinase activity and PknG-mediated virulence. PknG-mediated phosphorylation of universal (canonical) substrates such as Mbp and histone HIIA fractions was poor compared with the other characterized *M. tuberculosis* STPKs. We found that GarA, a homolog of CgPknG substrate OdhI, is a robust substrate of *M. tuberculosis* PknG, as GarA is phosphorylated with at least 10-fold higher efficiency than the canonical substrates (Fig. 1). O'Hare *et al.* (12) reported that PknG-mediated phosphorylation of GarA regulates glutamate metabolism in mycobacteria. This work is an attempt to understand the importance of the N- and C-terminal domains that sandwich the kinase domain of PknG, wherein GarA has been used as a substrate for all biochemical analyses.

The C-terminal TPR domain, a helical coiled-coil structure, reported to be present in proteins involved in signaling pathways (50) is known to play a role in arbitrating protein-protein interactions (51). Results showed that deleting the TPR domain decreased kinase activity by 80% (Table 1). Although the N-terminal deletion mutants (see Fig. 2 and Table 1; PknG-(151–750) and –(74–750)) showed a severely compromised activity, we observed that these mutants could bind ATP (supplemental Fig. S2), suggesting that the loss of activity may be due to the lack of an essential regulatory function. The Trx-fold, a structural motif consisting of a four-stranded β sheet and three flanking α helices, has been implicated in regulating various functions including iron/cadmium binding, maintaining the protein in-folded state, and in sensing the redox state of the environment (52). Although the sequence similarity between various proteins that contain this fold is minimal, they are present in most redox proteins. The active site motif C*XX*C is conserved

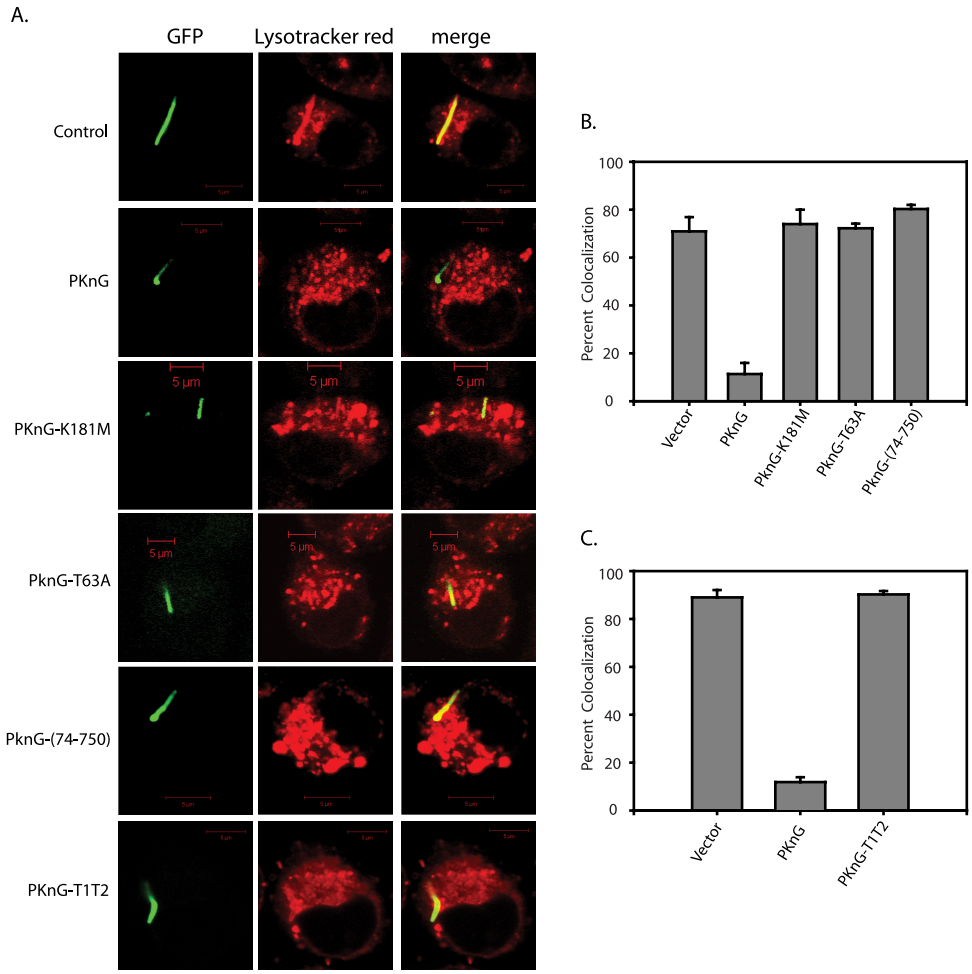

FIGURE 8. **The N-terminal region of PknG, threonine 63, and the Trx region mediate the survival of mycobacteria in host macrophages.** *M. smegmatis* expressing GFP was transformed with pVV16, pVV16-PknG, pVV16-PknG-K181M, pVV16-PknG-(74–750), pVV16-PknG-T63A, or pVV16-PknG-T1T2. J774A.1 cells plated on the coverslip were infected at an multiplicity of infection of 1:10 with GFP-*M. smegmatis* transformants, for 1 h. Three hours post-infection cells were stained with lysotracker red, fixed, and mounted. *A*, *panels in first column*, GFP-*M.* smegmatis expressing various mutants of PknG. *Panels in second column*, lysotracker red staining to mark acidic compartments. *Panels in third column*, co-localization of *M. smegmatis* with the lysosomal compartment of cell. The images shown are representative images taken 3 h post-infection using a Carl Zeiss Axiovision LSM510 meta confocal microscope. *B* and *C*, graph depicting the percent of GFP-*M. smegmatis* expressing PknG or PknG mutants that co-localize with lysotracker red. Images were procured using a Carl Zeiss Imager M1 fluorescence microscope. Twenty-five fields were counted for each sample and the percent co-localization was calculated as (GFP co-localized with lysotracker red/total number of infected cells that were counted) × 100. Values obtained from two independent experiments were used for calculating the mean ± S.E.

across all these proteins (52). The Trx-fold in PknG was suggested to be a characteristic ruberedoxin domain involved in iron binding (32). We carried out an iron staining experiment with purified PknG and PknG-T1T2 mutant, using ferritin as the positive control as described (53). Although we could detect staining of ferritin, PknG and PknG-T1T2 did not show any iron staining (data not shown), which suggested that the role of the Trx-fold in PknG is not that of iron binding. Results shown in Fig. 3 demonstrate that the PknG kinase activity is sensitive to the redox environment, and mutating the conserved cysteines to alanines results in abrogation of this response. In contrast to a previous report (32), where simultaneous mutations of these conserved cysteines to serines resulted in an inactive kinase, we observed that the PknG-T1T2 mutant retained ~40–50% activity (Fig. 3). This disparity in the results could be due the fact that we mutated cysteine residues to alanine and not to serine.

Serine/threonine kinases are classified into two categories, RD kinases and non-RD kinases, depending on the presence or absence of an arginine residue next to the conserved aspartate residue in the catalytic loop (54). RD kinases are known to be phosphorylated on their activation segment, which includes the β helix, activation loop, and the $p + 1$ loop. Primary phosphorylation on the activation segment occurs in the activation loop and in some cases secondary phosphorylation is known to occur in the $p + 1$ loop (55). Among mycobacterial kinases, phosphorylation in the activation loop has been reported in the case of PknA, -B, -E, -D, and -F. In PknE, an additional phosphorylation has been detected on the threonine residue in the $p + 1$ loop (49, 56). The crystal structure of PknG shows a stable activation loop, suggesting the lack of phosphorylation in the activation loop (32). The phosphoamino acid analysis revealed that PknG is exclusively phosphorylated on threonine residues (Fig. 1*D*), but the activation loop of PknG lacks threonine residues. Hence, we investigated the possibility of the site of phosphorylation being threonine 309 in the $p + 1$ loop of PknG. However, mutational analysis clearly showed that threonine 309 in PknG is not phosphorylated (Fig. 4). Interestingly, our results show that the hydroxyl group on threonine 309 is crucial for PknG activity, suggesting a role in arbitrating interactions with the substrate, or in stabilization of the activation segment.

We found PknG to phosphorylate the N-terminal Trx domain (PknG-Trx) (Fig. 6) an observation that is in agreement with previous findings (32). *In vitro* experiments revealed Thr-63 to be the major phosphorylation site in the N-terminal region (Fig. 6). With the help of mass spectrometry two groups (12, 57) have determined, Thr-21, Thr-23, Thr-26, Thr-32, Thr-63, Thr-64, and Ser-65 to be sites of phosphorylation in PknG. In addition, they have found that PknGΔ73 (which lacks N-terminal 73 amino acids) is not phosphorylated, and suggest that all phosphorylation sites lie within the N-terminal 73 amino acids. In contrast, we detected phosphorylation of PknG-(74–750), *i.e.* PknGΔ73 (Fig. 2), albeit at lower levels compared with PknG, suggesting additional phosphorylation

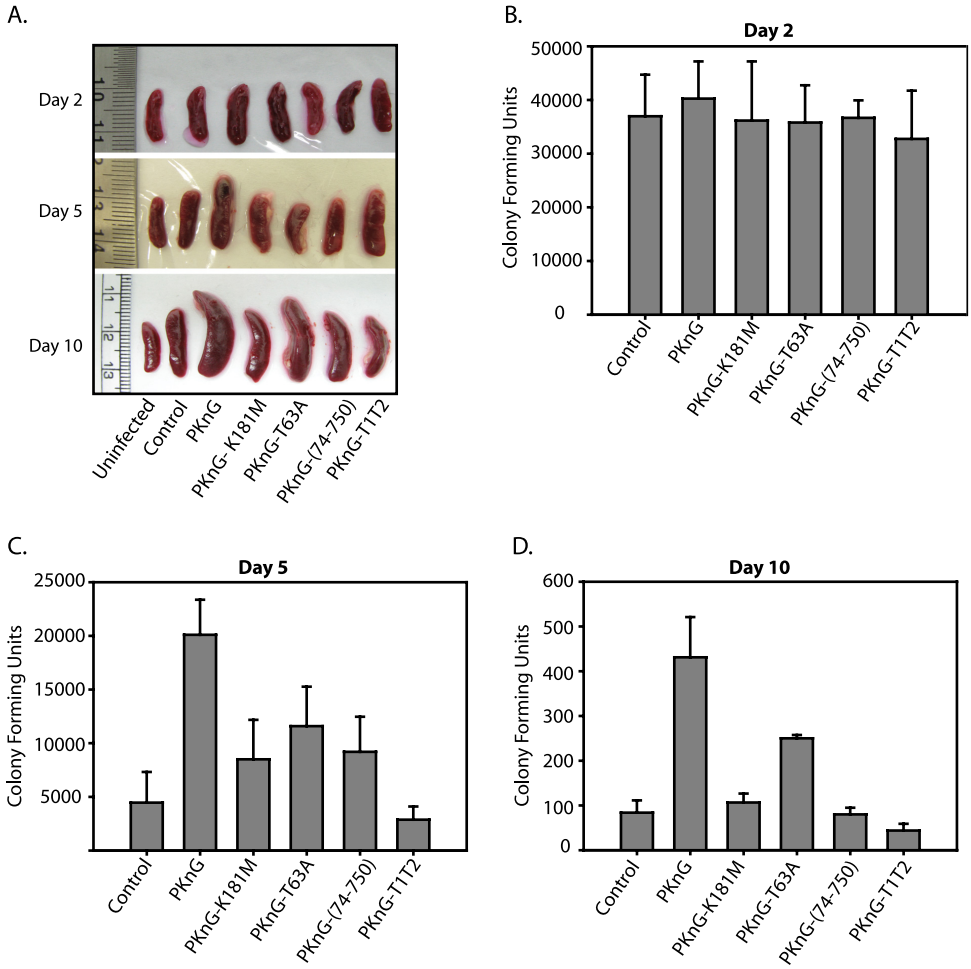

FIGURE 9. **Survival of *M. smegmatis* expressing wild type or mutant PknG in mouse tissue.** Groups of three mice were injected with *M. smegmatis* containing vector only (control) or expressing PknG, PknG-K181M, PknG-T63A, PknG-(74–750), and PknG-T1T2. *Panel A* compares the spleen size of the mice infected as described above with the spleen from an uninfected mouse. *B–D*, the CFUs obtained from spleen on days 2, 5, and 10. The above result is an average of three independent experiments and the mean ± S.E. is presented as *error bars*.

sites elsewhere. This result is in agreement with an earlier report that suggested phosphorylation of the C-terminal TPR domain (35). Although PknG phosphorylates various residues in the N-terminal region *in vitro*, metabolic labeling experiments with *M. smegmatis* expressing various PknG constructs have unambiguously revealed that Thr-63 is the only phosphorylation site *in vivo* (Fig. 7). Interestingly, we observed *in vivo* phosphorylation of kinase-inactive PknG (PknG-K181M) as well, suggesting phosphorylation of PknG by other serine/threonine kinase(s).

The role of an active form of PknG in the continued existence of *M. bovis* BCG in macrophages by evasion of lysosomal fusion has been well documented (37, 57). Our study presents data indicating the importance of the first 73 amino acids in PknG-mediated evasion of the lysosomal transfer of mycobacteria. These results are in agreement with a recent report where the authors have obtained similar results by overexpressing the PknGΔ73 mutant in *M. bovis* BCG (57). Most importantly, our results definitively demonstrate the essential role of threonine 63, the only *in vivo* phosphorylation site of PknG, in modulating the survival of the microbe in its host. Thus phosphorylation on Thr-63 is an important mode of regulation of the PknG activity. In addition, results also reveal a prominent role for conserved cysteines in the Trx motif. This motif also seems to be essential for regulating PknG-mediated survival of mycobacteria (see Figs. 8 and 9), thus suggesting a correlation between the role of the Trx motifs present in sensing the redox environment and PknG-mediated survival of mycobacteria.

Upon infecting mice with recombinant *M. smegmatis* we found that the expression of PknG in *M. smegmatis* brings about a marked difference in pathogenicity and its survival within the host. A significantly enlarged spleen and higher CFUs in mice infected with the *M. smegmatis* strain expressing PknG, as compared with the wild type *M. smegmatis,* points toward a stronger inflammatory response against the pathogen in the host, and a role for PknG in the persistence of the pathogenic mycobacteria in host tissues after an initial inflammatory response. The fact that none of the mutants could survive in mice spleen as effectively as strains expressing PknG underlines the importance of these residues in PknG mediating its effect. Thus, the N-terminal 73-amino acid region of PknG, the conserved Trx motifs of PknG, and the phosphorylation on Thr-63 are independently essential for *in vitro* and *in vivo* functioning of PknG. Future investigations will be aimed at understanding the PknG signaling cascade and determine the role played by other STPKs in modulating PknG-mediated survival of mycobacteria in the host.

Acknowledgments—We thank TBVRM for providing the shuttle vector pVV16, Dr. Y. Singh for the pGEX5X3-PknG-K181M construct, and Dr. Stewart Cole for providing the M. tuberculosis BAC library. We also thank Kalpana Rajanala for assistance with confocal microscopy. The animal experiments were done following the norms and procedures approved by the Institutional Animal Ethics Committee, National Institute of Immunology, New Delhi, India.

REFERENCES

1. Cole, S. T., Brosch, R., Parkhill, J., Garnier, T., Churcher, C., Harris, D., Gordon, S. V., Eiglmeier, K., Gas, S., Barry, C. E., 3rd, Tekaia, F., Badcock, K., Basham, D., Brown, D., Chillingworth, T., Connor, R., Davies, R., Devlin, K., Feltwell, T., Gentles, S., Hamlin, N., Holroyd, S., Hornsby, T., Jagels, K., Krogh, A., McLean, J., Moule, S., Murphy, L., Oliver, K., Osborne, J., Quail, M. A., Rajandream, M. A., Rogers, J., Rutter, S., Seeger, K., Skelton,

J., Squares, R., Squares, S., Sulston, J. E., Taylor, K., Whitehead, S., and Barrell, B. G. (1998) *Nature* **393,** 537–544
2. Av-Gay, Y., and Everett, M. (2000) *Trends Microbiol.* **8,** 238–244
3. Kumar, P., Kumar, D., Parikh, A., Rananaware, D., Gupta, M., Singh, Y., and Nandicoori, V. K. (2009) *J. Biol. Chem.* **284,** 11090–11099
4. Chaba, R., Raje, M., and Chakraborti, P. K. (2002) *Eur. J. Biochem.* **269,** 1078–1085
5. Av-Gay, Y., Jamil, S., and Drews, S. J. (1999) *Infect. Immun.* **67,** 5676–5682
6. Peirs, P., Parmentier, B., De Wit, L., and Content, J. (2000) *FEMS Microbiol. Lett.* **188,** 135–139
7. Molle, V., Girard-Blanc, C., Kremer, L., Doublet, P., Cozzone, A. J., and Prost, J. F. (2003) *Biochem. Biophys. Res. Commun.* **308,** 820–825
8. Koul, A., Choidas, A., Tyagi, A. K., Drlica, K., Singh, Y., and Ullrich, A. (2001) *Microbiology* **147,** 2307–2314
9. Molle, V., Kremer, L., Girard-Blanc, C., Besra, G. S., Cozzone, A. J., and Prost, J. F. (2003) *Biochemistry* **42,** 15300–15309
10. Lakshminarayan, H., Narayanan, S., Bach, H., Sundaram, K. G., and Av-Gay, Y. (2008) *Protein Expr. Purif.* **58,** 309–317
11. Gopalaswamy, R., Narayanan, P. R., and Narayanan, S. (2004) *Protein Expr. Purif.* **36,** 82–89
12. O'Hare, H. M., Durán, R., Cerveñansky, C., Bellinzoni, M., Wehenkel, A. M., Pritsch, O., Obal, G., Baumgartner, J., Vialaret, J., Johnsson, K., and Alzari, P. M. (2008) *Mol. Microbiol.* **70,** 1408–1423
13. Parikh, A., Verma, S. K., Khan, S., Prakash, B., and Nandicoori, V. K. (2009) *J. Mol. Biol.* **386,** 451–464
14. Cohen-Gonsaud, M., Barthe, P., Canova, M. J., Stagier-Simon, C., Kremer, L., Roumestand, C., and Molle, V. (2009) *J. Biol. Chem.* **284,** 19290–19300
15. Veyron-Churlet, R., Molle, V., Taylor, R. C., Brown, A. K., Besra, G. S., Zanella-Cléon, I., Fütterer, K., and Kremer, L. (2009) *J. Biol. Chem.* **284,** 6414–6424
16. Park, S. T., Kang, C. M., and Husson, R. N. (2008) *Proc. Natl. Acad. Sci. U.S.A.* **105,** 13105–13110
17. Thakur, M., and Chakraborti, P. K. (2008) *Biochem. J.* **415,** 27–33
18. Canova, M. J., Veyron-Churlet, R., Zanella-Cleon, I., Cohen-Gonsaud, M., Cozzone, A. J., Becchi, M., Kremer, L., and Molle, V. (2008) *Proteomics* **8,** 521–533
19. Canova, M. J., Kremer, L., and Molle, V. (2009) *J. Bacteriol.* **191,** 2876–2883
20. Greenstein, A. E., Grundner, C., Echols, N., Gay, L. M., Lombana, T. N., Miecskowski, C. A., Pullen, K. E., Sung, P. Y., and Alber, T. (2005) *J. Mol. Microbiol. Biotechnol.* **9,** 167–181
21. Gopalaswamy, R., Narayanan, S., Jacobs, W. R., Jr., and Av-Gay, Y. (2008) *FEMS Microbiol. Lett.* **278,** 121–127
22. Gopalaswamy, R., Narayanan, S., Chen, B., Jacobs, W. R., and Av-Gay, Y. (2009) *FEMS Microbiol. Lett.* **295,** 23–29
23. Houben, E. N., Walburger, A., Ferrari, G., Nguyen, L., Thompson, C. J., Miess, C., Vogel, G., Mueller, B., and Pieters, J. (2009) *Mol. Microbiol.* **72,** 41–52
24. Thakur, M., and Chakraborti, P. K. (2006) *J. Biol. Chem.* **281,** 40107–40113
25. Kang, C. M., Abbott, D. W., Park, S. T., Dascher, C. C., Cantley, L. C., and Husson, R. N. (2005) *Genes Dev.* **19,** 1692–1704
26. Deol, P., Vohra, R., Saini, A. K., Singh, A., Chandra, H., Chopra, P., Das, T. K., Tyagi, A. K., and Singh, Y. (2005) *J. Bacteriol.* **187,** 3415–3420
27. Sharma, K., Gupta, M., Pathak, M., Gupta, N., Koul, A., Sarangi, S., Baweja, R., and Singh, Y. (2006) *J. Bacteriol.* **188,** 2936–2944
28. Greenstein, A. E., Echols, N., Lombana, T. N., King, D. S., and Alber, T. (2007) *J. Biol. Chem.* **282,** 11427–11435
29. Ortiz-Lombardía, M., Pompeo, F., Boitel, B., and Alzari, P. M. (2003) *J. Biol. Chem.* **278,** 13094–13100
30. Young, T. A., Delagoutte, B., Endrizzi, J. A., Falick, A. M., and Alber, T. (2003) *Nat. Struct. Biol.* **10,** 168–174
31. Gay, L. M., Ng, H. L., and Alber, T. (2006) *J. Mol. Biol.* **360,** 409–420
32. Scherr, N., Honnappa, S., Kunz, G., Mueller, P., Jayachandran, R., Winkler, F., Pieters, J., and Steinmetz, M. O. (2007) *Proc. Natl. Acad. Sci. U.S.A.* **104,** 12151–12156
33. Good, M. C., Greenstein, A. E., Young, T. A., Ng, H. L., and Alber, T. (2004) *J. Mol. Biol.* **339,** 459–469
34. Mieczkowski, C., Iavarone, A. T., and Alber, T. (2008) *EMBO J.* **27,** 3186–3197
35. Cowley, S., Ko, M., Pick, N., Chow, R., Downing, K. J., Gordhan, B. G., Betts, J. C., Mizrahi, V., Smith, D. A., Stokes, R. W., and Av-Gay, Y. (2004) *Mol. Microbiol.* **52,** 1691–1702
36. Nguyen, L., Walburger, A., Houben, E., Koul, A., Muller, S., Morbitzer, M., Klebl, B., Ferrari, G., and Pieters, J. (2005) *J. Bacteriol.* **187,** 5852–5856
37. Walburger, A., Koul, A., Ferrari, G., Nguyen, L., Prescianotto-Baschong, C., Huygen, K., Klebl, B., Thompson, C., Bacher, G., and Pieters, J. (2004) *Science* **304,** 1800–1804
38. Stanley, S. A., Raghavan, S., Hwang, W. W., and Cox, J. S. (2003) *Proc. Natl. Acad. Sci. U.S.A.* **100,** 13001–13006
39. Finlay, B. B., and Falkow, S. (1997) *Microbiol. Mol. Biol. Rev.* **61,** 136–169
40. Fiuza, M., Canova, M. J., Zanella-Cléon, I., Becchi, M., Cozzone, A. J., Mateos, L. M., Kremer, L., Gil, J. A., and Molle, V. (2008) *J. Biol. Chem.* **283,** 18099–18112
41. Boyle, W. J., van der Geer, P., and Hunter, T. (1991) *Methods Enzymol.* **201,** 110–149
42. Collins, F. M. (1985) *Tubercle* **66,** 267–276
43. Dheenadhayalan, V., Delogu, G., and Brennan, M. J. (2006) *Microbes. Infect.* **8,** 262–272
44. Niebisch, A., Kabus, A., Schultz, C., Weil, B., and Bott, M. (2006) *J. Biol. Chem.* **281,** 12300–12307
45. Weldingh, K., Rosenkrands, I., Jacobsen, S., Rasmussen, P. B., Elhay, M. J., and Andersen, P. (1998) *Infect. Immun.* **66,** 3492–3500
46. Villarino, A., Duran, R., Wehenkel, A., Fernandez, P., England, P., Brodin, P., Cole, S. T., Zimny-Arndt, U., Jungblut, P. R., Cerveñansky, C., and Alzari, P. M. (2005) *J. Mol. Biol.* **350,** 953–963
47. Grundner, C., Gay, L. M., and Alber, T. (2005) *Protein Sci.* **14,** 1918–1921
48. Thakur, M., Chaba, R., Mondal, A. K., and Chakraborti, P. K. (2008) *J. Biol. Chem.* **283,** 8023–8033
49. Durán, R., Villarino, A., Bellinzoni, M., Wehenkel, A., Fernandez, P., Boitel, B., Cole, S. T., Alzari, P. M., and Cerveñansky, C. (2005) *Biochem. Biophys. Res. Commun.* **333,** 858–867
50. Das, A. K., Cohen, P. W., and Barford, D. (1998) *EMBO J.* **17,** 1192–1199
51. Cortajarena, A. L., and Regan, L. (2006) *Protein Sci.* **15,** 1193–1198
52. Martin, J. L. (1995) *Structure* **3,** 245–250
53. Raghunand, T. R., and Bishai, W. R. (2006) *J. Bacteriol.* **188,** 6966–6976
54. Krupa, A., and Srinivasan, N. (2005) *BMC Genomics* **6,** 129
55. Nolen, B., Taylor, S., and Ghosh, G. (2004) *Mol. Cell* **15,** 661–675
56. Molle, V., Zanella-Cleon, I., Robin, J. P., Mallejac, S., Cozzone, A. J., and Becchi, M. (2006) *Proteomics* **6,** 3754–3766
57. Scherr, N., Muller, P., Perisa, D., Combaluzier, B., Jeno, P., and Pieters, J. (2009) *J. Bacteriol.* **191,** 4546–4554

Key Residues in *Mycobacterium tuberculosis* Protein Kinase G Play a Role in Regulating Kinase Activity and Survival in the Host

Divya Tiwari, Rajnish Kumar Singh, Kasturi Goswami, Sunil Kumar Verma, Balaji Prakash and Vinay Kumar Nandicoori

J. Biol. Chem. 2009, 284:27467-27479.
doi: 10.1074/jbc.M109.036095 originally published online July 28, 2009
